Robustness to noise of distributed averaging integral controllers in power networks

Weitenberg, Erik; De Persis, Claudio

Published in:
Systems & Control Letters

DOI:
10.1016/j.sysconle.2018.06.003

Systems & Control Letters 119 (2018) 1–7

Contents lists available at ScienceDirect

Systems & Control Letters

journal homepage: www.elsevier.com/locate/sysconle

Robustness to noise of distributed averaging integral controllers in power networks ☆

Erik Weitenberg *, Claudio De Persis

Engineering and Technology Institute Groningen and Jan Willems Center for Systems and Control, University of Groningen, 9747 AG Groningen, The Netherlands

ARTICLE INFO

Article history:
Received 9 January 2018
Received in revised form 2 May 2018
Accepted 17 June 2018
Available online 10 July 2018

Keywords:
Lyapunov methods
Networked systems
Power networks
Robustness analysis
Cyber–physical systems

ABSTRACT

We investigate the robustness of distributed averaging integral controllers for optimal frequency regulation of power networks to noise in measurements, communication and actuation. Specifically, using Lyapunov techniques, we show a property related to input-to-state stability of the closed loop system with respect to this noise. Using this result, a tuning trade-off between controller performance and noise rejection is highlighted.

1. Introduction

The modern AC power system balances supply and demand in real time despite faults and fluctuations in demand, supply and transport. Adequate control techniques on the supply side ensure all units on the network enjoy a stable voltage amplitude and frequency, which is critical for safety and performance. Traditionally, these challenges have been addressed using centralized control on multiple time scales, exploiting the large inertia in generation units to compensate for the relatively small effect of fluctuations and faults.

Recently, increasing prevalence of renewable low-inertia generation units has increased volatility of supply on small and large time scales. Additionally, the emergence of so-called microgrids has introduced the compelling case of a small-scale network that can operate independently of the larger power grid, relying on small local generators. Inspired by this, an active research area has emerged to deal with this volatility in a decentralized and flexible way.

This work focuses on the secondary control layer. Various approaches for secondary control have been taken in recent years, for example primal–dual methods [1–3], internal-model control [4,5] and distributed averaging integral (DAI) control [6–8,5]. We investigate the latter approach.

Previously the performance of the DAI controller has been addressed e.g. by Flamme et al. [9], who derived a $\mathcal{H}_2$-optimum for the controller parameters under measurement noise. Similarly, Wu et al. [10] use $\mathcal{H}_2$ techniques to find the optimal communication topology for the DAI controller. Additionally, Andreasson et al. [11] performed an analysis of the linearized system. In the present work however, we additionally consider frequency noise, and provide a stability certificate for the non-linear system instead of a linearized one. This has the additional advantage of making the work applicable to other systems with similar strongly convex dynamics.

1.1. Main contribution

To our knowledge, while the DAI controller offers stability [5] and exponential convergence [12], its robustness to noise in frequency measurements, actuation and communication has not been formally established. Recently, it was shown that the so-called *leaky integral controller* offers attractive robustness properties and tuning opportunities, though it lacks exact frequency regulation [13]. In this work, we show that the DAI controller in fact satisfies an input-to-state stability with restrictions property and robustness with respect to measurement noise, and for completeness also to actuation and communication noise. The analysis builds on results from Weitenberg et al. [12], but the ISS-with restrictions result pursued in this paper, as opposed to the exponential stability

☆ This work was partially supported by the NWO-URSES project ENBARK (Grant number is 408-13-037), the DST-NWO IndoDutch Cooperation on "Smart Grids - Energy management strategies for interconnected smart microgrids" and the STW Perspectief program "Robust Design of Cyber–physical Systems" –"Energy Autonomous Smart Microgrids".

* Corresponding author.
E-mail addresses: e.r.a.weitenberg@rug.nl (E. Weitenberg), c.de.persis@rug.nl (C. De Persis).

https://doi.org/10.1016/j.sysconle.2018.06.003
0167-6911/

result from Weitenberg et al. [12], requires to extend these results to the presence of disturbances and eventually show that the Lyapunov function proposed in Weitenberg et al. [12] is indeed an ISS-Lyapunov function. The result obtained is analogous to the result obtained in Weitenberg et al. [13] for the leaky integral controller, but the use of the distributed averaging controllers considered in this paper calls for a Lyapunov function different from Weitenberg et al. [13], which requires some adjustments in the analysis. Moreover, we show how this result can be exploited in the choice of tuning parameters for the controllers, highlighting a trade-off between robustness to noise and speedy response to fluctuations in demand. This makes the DAI controller a well-performing and comparably robust alternative to the leaky integral controller, *if a communication network is available.*

The remainder of this paper is organized as follows. In Section 2, the power network model is introduced, as well as the control objectives and the DAI controller. The energy function used to analyze the closed-loop system is introduced, along with its various properties, in Section 3. In Section 4, we exploit this energy function to derive a robustness property of the closed-loop system. This leads to an interesting trade-off between robustness and performance, which is highlighted in Section 5.

2. Setting

The power network is viewed as a graph $\mathcal{G} = (\mathcal{V}, \mathcal{E})$. The systems at the nodes are partitioned into a set of $n_{\mathbf{G}}$ generators and a set of $n_{\mathbf{L}}$ loads, with $n = n_{\mathbf{G}} + n_{\mathbf{L}}$. As such, $\mathcal{V} = \mathcal{V}_{\mathbf{G}} \cup \mathcal{V}_{\mathbf{L}}$. The graph's edges represent the m physical power lines between the various power systems.

We denote the $n \times m$ incidence matrix of $\mathcal{G}$ by $\mathcal{B}$. Without loss of generality, we assume the first $n_{\mathbf{G}}$ rows of $\mathcal{B}$ correspond to the generator nodes and the others to the loads. Accordingly, we write $\mathcal{B}^\top = [\mathcal{B}_{\mathbf{G}}^\top, \mathcal{B}_{\mathbf{L}}^\top]$.

We model the power network using the Bergen–Hill equations [14,15].

$$\dot{\theta}_{\mathbf{G}} = \omega_{\mathbf{G}} \tag{1a}$$

$$M_{\mathbf{G}}\dot{\omega}_{\mathbf{G}} = -D_{\mathbf{G}}\omega_{\mathbf{G}} - \mathcal{B}_{\mathbf{G}}\Gamma \sin(\mathcal{B}^\top\theta) + u \tag{1b}$$

$$D_{\mathbf{L}}\dot{\theta}_{\mathbf{L}} = -\mathcal{B}_{\mathbf{L}}\Gamma \sin(\mathcal{B}^\top\theta) - P. \tag{1c}$$

Here, $\theta \in \mathbb{R}^n$ denotes the vector of voltage angles of the synchronous machines and loads at the nodes, relative to a frame of reference rotating at a nominal frequency ω^*, usually 50 or 60 Hz. Likewise, $\omega \in \mathbb{R}^n$ denotes a machine's frequency deviation from ω^*. D and M are diagonal $n \times n$ matrices encoding the droop gain and inertia at each node respectively, with the understanding that inertia at the load nodes is zero. As with $\mathcal{B}$, the subscript $_{\mathbf{G}}$ and $_{\mathbf{L}}$ denote partition of vectors and (diagonal) matrices into source and load nodes, i.e. $\theta = [\theta_{\mathbf{G}}^\top, \theta_{\mathbf{L}}^\top]^\top$, $\omega = [\omega_{\mathbf{G}}^\top, \omega_{\mathbf{L}}^\top]^\top$, $M = \text{block diag}(M_{\mathbf{G}}, M_{\mathbf{L}})$ et cetera. Γ is a diagonal $m \times m$ matrix encoding the susceptance B_k of the power lines and the voltage amplitudes V_i and V_j at each edge as $\Gamma_{kk} = B_k V_i V_j$, for each edge $k = (i,j) \in \mathcal{E}$. Finally, $u \in \mathbb{R}^{n_{\mathbf{G}}}$ is the control input and $P \in \mathbb{R}^{n_{\mathbf{L}}}$ is the demand at the load nodes. In the Bergen–Hill model, these load nodes are assumed to be dynamic as opposed to static impedance loads, which are subsequently absorbed into the line susceptances in a reduced network [14].

For ease of analysis, we will use the following equivalent form of (1), in which we introduce the potential function $U(\theta) = -\mathbb{1}^\top \Gamma \cos(\mathcal{B}^\top\theta)$:

$$\dot{\theta} = \omega \tag{2a}$$

$$M_{\mathbf{G}}\dot{\omega}_{\mathbf{G}} = -D_{\mathbf{G}}\omega_{\mathbf{G}} - \nabla U(\theta)_{\mathbf{G}} + u \tag{2b}$$

$$\mathbb{0} = -D_{\mathbf{L}}\omega_{\mathbf{L}} - \nabla U(\theta)_{\mathbf{L}} - P. \tag{2c}$$

Remark 1. The analysis in this paper of the behavior of the DAI controller is not limited to the swing equations seen in power networks, but to a large class of nonlinear passive networks [16]. In fact, as long as the potential function U is strongly convex and the diagonal matrices $M_{\mathbf{G}}$ and D are positive definite, the results hold.

The generator nodes are controlled by distributed averaging integral controllers [17,5,18]. These controllers are equipped with a communication network $\mathcal{G}_u = (\mathcal{V}_{\mathbf{G}}, \mathcal{E}_u)$, consisting of all generator nodes and an edge set possibly different from that of $\mathcal{G}$. Under mild assumptions (detailed later) and noise-free circumstances, these controllers minimize a quadratic cost function $C(u) = \frac{1}{2}\sum_{i\in\mathcal{V}_{\mathbf{G}}} Q_i u_i^2$ while ensuring that $\sum_{i\in\mathbf{G}} u_i = \sum_{i\in\mathbf{L}} P_i$ [18]. This allows the user to guarantee economically optimal operation, in addition to frequency regulation.

We apply the DAI controller with measurement noise ν_1. Additionally, we allow for communication noise ν_2 to occur before transmission.

$$\dot{u}_i = -\sum_{j\in\mathcal{N}i} Q_i u_i - Q_j(u_j + \nu_{2,j}) - Q_i^{-1}(\omega_i + \nu_{1,i}). \tag{3}$$

We define the noise ν_ω so that both the measurement noise and the communication noise are encapsulated in it. That is, $\nu_{\omega,i} := \nu_{1,i} - \sum_{j\in\mathcal{N}i} Q_i Q_j \nu_{2,j}$. As a result, we write the controller in vector form as

$$\dot{u} = -\mathcal{L}_u Q u - Q^{-1}(\omega_{\mathbf{G}} + \nu_\omega). \tag{4}$$

The noise $\nu_\omega = \nu_\omega(t)$ is assumed to be an infinity-norm-bounded function of time. Likewise, and for the sake of completeness, we assume the control input contains noise, replacing (2b) by

$$M_{\mathbf{G}}\dot{\omega}_{\mathbf{G}} = -D_{\mathbf{G}}\omega_{\mathbf{G}} - \nabla U(\theta)_{\mathbf{G}} + u + \nu_u, \tag{5}$$

where again, $\nu_u = \nu_u(t)$ is an infinity-norm-bounded function of time.

For ease of analysis, we now apply a coordinate transformation on the rotor angles θ. Following [12,13], instead of these, we use the offset from the average of the angles, setting $\delta := \Pi\theta := (I - \frac{1}{n}\mathbb{1}\mathbb{1}^\top)\theta$. Note that $\mathcal{B}^\top\Pi = \mathcal{B}^\top$, as $\mathcal{B}^\top\mathbb{1} = \mathbb{0}$. We will commit a slight abuse of notation by using the symbol U to also refer to the potential as a function of δ.

2.1. Steady state analysis

The system (2) in closed loop with distributed averaging integral controllers is well studied [8,18,12]. In the noise-free case, the system converges exponentially to a synchronous solution $\bar{\delta}$, $\bar{\omega} = \mathbb{0}$, $\bar{u}$ satisfying

$$\mathbb{0} = -\nabla U(\bar{\delta}) + \text{col}(\bar{u}, -P) \tag{6}$$

$$\bar{u} = Q^{-1}\mathbb{1}_{\mathbf{G}}\frac{\mathbb{1}_{\mathbf{L}}^\top P}{\mathbb{1}_{\mathbf{G}}^\top Q^{-1}\mathbb{1}_{\mathbf{G}}}, \tag{7}$$

provided the following assumption holds:

Assumption 1 (*Feasibility*)**.** There exists a vector $\bar{\delta} \in \text{Im}\,\Pi$ such that (6)–(7) is satisfied. Moreover, there exists a $\rho \in \left(0, \frac{\pi}{2}\right)$ such that $\mathcal{B}^\top\bar{\delta}$ is in the *interior* of $\Theta := [\rho - \frac{\pi}{2}, \frac{\pi}{2} - \rho]^n$.

It will be convenient for later analysis to write the closed-loop system in incremental form [see e.g. 5], recalling that the notation $v_{\mathbf{G}}, v_{\mathbf{L}}$ is used to partition a vector v into subvectors for the sources and loads:

$$\dot{\delta} = \Pi\omega \tag{8a}$$

$$M_{\mathbf{G}}\dot{\omega}_{\mathbf{G}} = -D_{\mathbf{G}}\omega_{\mathbf{G}} - (\nabla U(\delta) - \nabla U(\bar{\delta}))_{\mathbf{G}} + u - \bar{u} + \nu_u \tag{8b}$$

$$\mathbb{0} = -D_{\mathbf{L}}\omega_{\mathbf{L}} - (\nabla U(\delta) - \nabla U(\bar{\delta}))_{\mathbf{L}} \tag{8c}$$

$$\dot{u} = -\mathcal{L}_u Q(u-\bar{u}) - Q^{-1}(\omega_{\mathbf{G}} + \nu_\omega). \tag{8d}$$

3. Lyapunov function

We use for this system the Lyapunov function

$$\begin{aligned} W &= W_0 + \epsilon_1 W_1 + \epsilon_2 W_2 \\ &:= U(\delta) - U(\bar{\delta}) - \nabla U(\bar{\delta})^\top(\delta - \bar{\delta}) \\ &\quad + \frac{1}{2}\omega^\top M\omega + \frac{1}{2}(u-\bar{u})Q(u-\bar{u}) \qquad (9a) \\ &\quad + \epsilon_1\omega^\top M(\nabla U(\delta) - \nabla U(\bar{\delta})) \\ &\quad - \epsilon_2\omega^\top M\mathbb{1}_n\mathbb{1}_{n_{\mathbf{G}}}^\top(u-\bar{u}) \qquad (9b) \end{aligned}$$

from Weitenberg et al. [12]. This Lyapunov function includes an energy-based component (9a) and two cross-terms (9b) that will make sure the Lyapunov function is strictly decreasing along solutions, as we will show in Lemma 2.

Lemma 1 (*Positivity of W [12]*). *Suppose Assumption 1 holds. There exist sufficiently small ϵ_1, ϵ_2 and positive constants $\underline{c}, \bar{c}$ such that for all δ with $\mathcal{B}^\top\delta \in \Theta$, we have*

$$\underline{c}\|x_{\mathbf{G}}(\delta,\omega_{\mathbf{G}},u)\|^2 \le W(\delta,\omega,u) \le \bar{c}\|x_{\mathbf{G}}(\delta,\omega_{\mathbf{G}},u)\|^2 \tag{10}$$

where $x_{\mathbf{G}}(\delta,\omega_{\mathbf{G}},u) := \operatorname{col}(\delta-\bar{\delta}, \omega_{\mathbf{G}}, u-\bar{u})$.

In fact,

$$\underline{c} = \tfrac{1}{2}\min\big(\lambda_{\min}(M_{\mathbf{G}}) - (\epsilon_1+\epsilon_2)\lambda_{\max}(M_{\mathbf{G}})^2, \lambda_{\min}(Q) - \epsilon_2 n^2, 2\beta_1 - \epsilon_1\alpha_2\big), \tag{11a}$$

$$\bar{c} = \tfrac{1}{2}\max\big(\lambda_{\max}(M_{\mathbf{G}}) + (\epsilon_1+\epsilon_2)\lambda_{\max}(M_{\mathbf{G}})^2, \lambda_{\max}(Q) + \epsilon_2 n^2, 2\beta_2 + \epsilon_1\alpha_2\big), \tag{11b}$$

where $\alpha_1, \alpha_2, \beta_1$ and β_2 are positive constants emerging from the proof of [12, Lemma 1 and Lemma 4].

3.1. Derivative of the Lyapunov function

We aim to show that W is strictly decreasing along solutions of (8). To this end, we first compute and bound the directional derivative of W with respect to the vector field (8).

Lemma 2. *There exists a positive scalar c' such that the directional derivative of W along the vector field (8) satisfies*

$$\begin{aligned}\dot{W} \le& -c'\|x(\delta,\omega,u)\|^2 \\ &- \nu_\omega^\top(u-\bar{u}-\epsilon_2 Q^{-1}\mathbb{1}_{n_{\mathbf{G}}}\mathbb{1}_n^\top M\omega) \\ &+ \nu_u^\top(\omega_{\mathbf{G}} + \epsilon_1(\nabla U(\delta) - \nabla U(\bar{\delta}))_{\mathbf{G}} \\ &\quad - \epsilon_2\mathbb{1}\mathbb{1}^\top(u-\bar{u})),\end{aligned} \tag{12}$$

with

$$x(\delta,\omega,u) := \operatorname{col}(\delta-\bar{\delta},\omega,u-\bar{u}). \tag{13}$$

Proof. The proof consists of three parts. First, we calculate the directional derivative of W along solutions to (8). Second, we write the derivative as a quadratic form, bounding it in terms of the norm of a vector. Finally, we write this bound in terms of the familiar state vector x.

The derivative of the orthodox part (9a) of W is

$$\begin{aligned}\dot{W}_0 =& (\nabla U(\delta) - \nabla U(\bar{\delta}))^\top \Pi\omega \\ &+ \omega_{\mathbf{G}}^\top(-D_{\mathbf{G}}\omega_{\mathbf{G}} - (\nabla U(\delta) - \nabla U(\bar{\delta}))_{\mathbf{G}} \\ &\quad + u - \bar{u} + \nu_u) \\ &+ \omega_{\mathbf{L}}^\top(-D_{\mathbf{L}}\omega_{\mathbf{L}} - (\nabla U(\delta) - \nabla U(\bar{\delta}))_{\mathbf{L}}) \\ &+ (u-\bar{u})^\top Q(-\mathcal{L}_u Q(u-\bar{u}) - Q^{-1}(\omega_{\mathbf{G}}+\nu_\omega)) \\ =& -\omega^\top D\omega - (u-\bar{u})^\top Q\mathcal{L}_u Q(u-\bar{u}) \\ &- (u-\bar{u})^\top\nu_\omega + \omega_{\mathbf{G}}^\top\nu_u\end{aligned} \tag{14a}$$

The first cross term has derivative

$$\begin{aligned}\dot{W}_1 =& \omega^\top M\nabla^2 U(\delta)\omega + (\nabla U(\delta) - \nabla U(\bar{\delta}))^\top \\ &\cdot(-D\omega - (\nabla U(\delta) - \nabla U(\bar{\delta})) \\ &+ \operatorname{col}(u-\bar{u}+\nu_u, \mathbb{0}_{\mathbf{L}}))\end{aligned} \tag{14b}$$

Finally, the second cross term has derivative

$$\begin{aligned}\dot{W}_2 =& \omega^\top M\mathbb{1}\mathbb{1}^\top Q^{-1}(\omega_{\mathbf{G}}+\nu_\omega) \\ &+ (u-\bar{u})^\top\mathbb{1}\mathbb{1}^\top(D\omega - \operatorname{col}(u-\bar{u}+\nu_u, \mathbb{0}_{\mathbf{L}}))\end{aligned} \tag{14c}$$

so the directional derivative of W becomes $\dot{W} = \dot{W}_0 + \epsilon_1\dot{W}_1 + \epsilon_2\dot{W}_2$.

We will now proceed to bound the derivative in terms of the vector

$$\chi(\delta,\omega,u) := \operatorname{col}(\nabla U(\delta) - \nabla U(\bar{\delta}), \omega, u-\bar{u}), \tag{15}$$

following the reasoning set forth in Weitenberg et al. [12, Lemma 3], but accounting for the fact that we do not have load-side controllers in the current scenario.

Collecting the terms of the directional derivative (14) yields

$$\begin{aligned}\dot{W}(\delta,\omega,u) =& -\chi(\delta,\omega,u)^\top K(\delta)\chi(\delta,\omega,u) \\ &- \nu_\omega^\top(u-\bar{u}) + \epsilon_2\nu_\omega^\top Q^{-1}\mathbb{1}_{n_{\mathbf{G}}}\mathbb{1}_n^\top M\omega \\ &+ \nu_u^\top(\omega_{\mathbf{G}} + \epsilon_1(\nabla U(\delta) - \nabla U(\bar{\delta}))_{\mathbf{G}} \\ &\quad - \epsilon_2\mathbb{1}\mathbb{1}^\top(u-\bar{u})),\end{aligned} \tag{16}$$

where

$$K(\delta) = \operatorname{sp}\begin{bmatrix}\epsilon_1 I & \epsilon_1 D & -\epsilon_1\operatorname{col}(I_{\mathbf{G}}, \mathbb{0}_{\mathbf{L}}) \\ \mathbb{0} & K_{22}(\delta) & -\epsilon_2 D\mathbb{1}_n\mathbb{1}_{n_{\mathbf{G}}}^\top \\ \mathbb{0} & \mathbb{0} & Q\mathcal{L}_u Q + \epsilon_2\mathbb{1}_{n_{\mathbf{G}}}\mathbb{1}_{n_{\mathbf{G}}}^\top\end{bmatrix}, \tag{17}$$

with $\operatorname{sp}(M) := \frac{1}{2}(M + M^\top)$ and $K_{22}(\delta) = D - \epsilon_1 M\nabla^2 U(\delta) - \epsilon_2 M\mathbb{1}_n\mathbb{1}_n^\top\operatorname{col}(Q^{-1}, \mathbb{0}_{\mathbf{L}})$.

Using the fact [12, Lemma 6] that for any submatrices a, b, c, d,

$$\begin{bmatrix} a & b^\top c \\ c^\top b & d\end{bmatrix} \ge \begin{bmatrix} a - b^\top b & 0 \\ 0 & d - c^\top c\end{bmatrix}, \tag{18}$$

we conclude that $K(\delta) \ge K'(\delta)$, where

$$\begin{aligned}K'(\delta) =& \operatorname{block\,diag}\Big(\frac{1}{2}\epsilon_1 I_{n_{\mathbf{G}}}, \\ &\operatorname{sp}K_{22}(\delta) - \epsilon_1 D^2 - \epsilon_2 n_{\mathbf{G}} D\mathbb{1}_n\mathbb{1}_n^\top D \\ &Q\mathcal{L}_u Q - (\epsilon_1 + \tfrac{1}{4}\epsilon_2)I_{n_{\mathbf{G}}} + \epsilon_2\mathbb{1}\mathbb{1}^\top\Big).\end{aligned} \tag{19}$$

We define c as the minimum eigenvalue of $K'(\delta)$, and note that it is strictly positive provided $\epsilon_1 \le \epsilon_2(n_{\mathbf{G}} - \frac{1}{4})$, and both ϵ_1 and ϵ_2 are sufficiently small that the middle block of (19) is positive definite.

As a result,

$$\begin{aligned}\dot{W} \le& -c\|\chi(\delta,\omega,u)\|^2 \\ &- \nu_\omega^\top(u-\bar{u}) + \epsilon_2\nu_\omega^\top Q^{-1}\mathbb{1}_{n_{\mathbf{G}}}\mathbb{1}_n^\top M\omega \\ &+ \nu_u^\top(\omega_{\mathbf{G}} + \epsilon_1(\nabla U(\delta) - \nabla U(\bar{\delta}))_{\mathbf{G}} \\ &\quad - \epsilon_2\mathbb{1}\mathbb{1}^\top(u-\bar{u})).\end{aligned} \tag{20}$$

For the final bound in terms of x, we now recall [12, Lemma 4] which states that there exists a positive scalar α_1 such that for all $\delta, \bar{\delta} \in \Theta$, $\|\nabla U(\delta) - \nabla U(\bar{\delta})\|^2 \geq \alpha_1 \|\delta - \bar{\delta}\|^2$. As a result, letting $c' = c \min(1, \alpha_1)$,

$$\begin{aligned}\dot{W} \leq & - c'\|x(\delta, \omega, u)\|^2 \\ & - \nu_\omega^\top (u - \bar{u}) + \epsilon_2 \nu_\omega^\top Q^{-1} \mathbb{1}_{n_\mathbf{G}} \mathbb{1}_n^\top M \omega \\ & + \nu_u^\top (\omega_\mathbf{G} + \epsilon_1 (\nabla U(\delta) - \nabla U(\bar{\delta}))_\mathbf{G} \\ & - \epsilon_2 \mathbb{1}\mathbb{1}^\top (u - \bar{u})). \quad \square\end{aligned}$$

Next, it is convenient to bound the cross terms involving the noise in (12) by quadratic expressions of the noise only, so we can discuss their individual effect in the following exposition. To this end, note that we can write (14) as

$$\begin{aligned}\dot{W} \leq & -c'\|x(\delta, \omega, u)\|^2 \\ & + \chi(\delta, \omega, u)^\top E_\omega \nu_\omega + \chi(\delta, \omega, u)^\top E_u \nu_u,\end{aligned} \tag{21}$$

with χ as in (15) and

$$E_\omega := \begin{bmatrix} \mathbb{0} \\ \epsilon_2 Q^{-1} \mathbb{1}\mathbb{1}^\top M \\ -I \end{bmatrix}, \quad E_u := \begin{bmatrix} \epsilon_1 I \\ I \\ -\epsilon_2 \mathbb{1}\mathbb{1}^\top \end{bmatrix} \tag{22}$$

Lemma 3. *There exist positive constants μ_0, μ_1 such that for all values of ν_ω, ν_u and x,*

$$\begin{aligned}&\chi(\delta, \omega, u)^\top E_\omega \nu_\omega + \chi(\delta, \omega, u)^\top E_u \nu_u \leq \\ &\quad \mu_0 \|x(\delta, \omega, u)\|^2 + \mu_1 \|\nu_\omega\|^2 + \mu_2 \|\nu_u\|^2,\end{aligned} \tag{23}$$

and $c' - \mu_0 > 0$.

Proof. Note that for arbitrary vectors a and b and an arbitrary positive constant μ,

$$\left\|\mu^{-\frac{1}{2}} a - \mu^{\frac{1}{2}} b\right\|^2 = \left(\mu^{-\frac{1}{2}} a - \mu^{\frac{1}{2}} b\right)^\top \left(\mu^{-\frac{1}{2}} a - \mu^{\frac{1}{2}} b\right) > 0.$$

Therefore, $2a^\top b \leq \mu^{-1}\|a\|^2 + \mu\|b\|^2$. We apply this to the left hand side of (23), which yields

$$\chi^\top E_\omega \nu_\omega \leq \frac{1}{2\mu} \|\chi\|^2 + \frac{\mu}{2} \|E_\omega \nu_\omega\|^2, \tag{24}$$

and likewise for the second term. Bounding $\|E_\omega \nu_\omega\|^2 \leq \lambda_{\max}(E_\omega^\top E_\omega)$ $\|\nu_\omega\|^2$, likewise for ν_u, and $\|\chi\|^2 \leq \max(1, \alpha_2)\|x\|^2$, where α_2 is a positive scalar derived using [12, Lemma 4] we see that (23) holds, for any value of μ, with $\mu_0 = \max(1, \alpha_2)/(2\mu)$,

$$\mu_1 := \frac{\mu}{2} \lambda_{\max}(E_\omega^\top E_\omega) \quad \text{and} \quad \mu_2 := \frac{\mu}{2} \lambda_{\max}(E_u^\top E_u). \tag{25}$$

To ensure that $c' - \mu_0 > 0$, we restrict the possible values of μ to the ones satisfying $\mu > \frac{\max(1,\alpha_2)}{2c'}$. $\square$

Combining Lemmas 2 and 3, we end up with the exponential bound

$$\begin{aligned}\dot{W} \leq & -(c' - \mu_0)\|x(\delta, \omega, u)\|^2 \\ & + \mu_1 \|\nu_\omega\|^2 + \mu_2 \|\nu_u\|^2.\end{aligned} \tag{26}$$

4. Main result

Having defined a Lyapunov function that is strictly decreasing along solutions to the system without measurement noise, we will be able to derive a result along the lines of input-to-state stability. First, we make explicit the stability criterion that is to be verified, already considered in [13].

Definition 1. A system $\dot{x} = f(x, \nu)$ is called input-to-state stable (ISS) with restriction X on $x(0)$ and restriction $N \in \mathbb{R}_{>0}$ on $\nu(\cdot)$, if there exist a class $\mathcal{KL}$-function β and a class $\mathcal{K}_\infty$-function γ such that for all $t \geq 0$, $x(0) \in X$ and all $\nu(\cdot) \in L_\infty^n$ satisfying

$$\|\nu(\cdot)\|_\infty := \operatorname*{ess\,sup}_{t \in \mathbb{R}_{>0}} \|\nu(t)\| \leq N, \tag{27}$$

we have

$$\|x(t)\| \leq \beta(\|x(0)\|, t) + \gamma(\|\nu(\cdot)\|_\infty). \tag{28}$$

Theorem 1 (*ISS of DAI-controlled Power System*)**.** *Consider the system (1) in closed-loop with the biased distributed integral controller (4) as described in (8). Let Assumption 1 hold. Then there exist positive constants N_1, N_2 and a set X such that the closed-loop system is ISS from the noise ν_ω, ν_u to the state $x(t) = x(\delta(t), \omega(t), u(t))$ with restrictions X on $x(0)$, N_1 on $\nu_\omega(\cdot)$ and N_2 on $\nu_u(\cdot)$. That is, there exist positive constants $\hat{\alpha}, \lambda$ and γ_1, γ_2 such that the solutions $x(t)$ for which $x(0) \in X$, $\|\nu_\omega(\cdot)\|_\infty \leq N_1$ and $\|\nu_u(\cdot)\|_\infty \leq N_2$ satisfy for all $t \geq 0$,*

$$\begin{aligned}\|x(t)\|^2 \leq & \lambda e^{-\hat{\alpha} t} \|x(0)\|^2 \\ & + \gamma_1 \|\nu_\omega(\cdot)\|_\infty^2 + \gamma_2 \|\nu_u(\cdot)\|_\infty^2.\end{aligned} \tag{29}$$

Proof. Combining Lemmas 2 and 3 yields

$$\begin{aligned}\dot{W}(t) &\leq -(c' - \mu_0)\|x(t)\|^2 + \mu_1 \|\nu_\omega(t)\|^2 + \mu_2 \|\nu_u(t)\|^2 \\ &\leq -(c' - \mu_0)\|x_\mathbf{G}(t)\|^2 + \mu_1 \|\nu_\omega(t)\|^2 + \mu_2 \|\nu_u(t)\|^2 \\ &\leq -\frac{c' - \mu_0}{\bar{c}} W(t) + \mu_1 \|\nu_\omega(t)\|^2 + \mu_2 \|\nu_u(t)\|^2,\end{aligned} \tag{30}$$

where the last inequality follows from Lemma 1. For the remainder of this proof, we set $\hat{\alpha} := 2\frac{c' - \mu_0}{\bar{c}}$.

Note that this relation holds only to the extent that $\delta \in \Theta$. As a result, we must require that X be the largest sublevel set $\Delta_w := \{x : W(x) \leq w\}$ for which $\mathcal{B}^\top \delta \in \Theta$. Given that $\mathcal{B}^\top \bar{\delta}$ is in the interior of Θ, X is nonempty and has an interior. To then ensure that the trajectories do not leave Δ_w, we note that on the boundary of Δ_w, (30) becomes

$$\begin{aligned}\dot{W} &\leq -\tfrac{1}{2}\hat{\alpha} w + \mu_1 \|\nu_\omega(t)\|^2 + \mu_2 \|\nu_u(t)\|^2 \\ &\leq -\tfrac{1}{2}\hat{\alpha} w + \mu_1 N_1 + \mu_2 N_2.\end{aligned}$$

Therefore, we require N_1, N_2 and w (and therefore X) be such that the condition $\dot{W} \leq 0$ is satisfied.

We now apply the Comparison Lemma [19, Lemma B.2] to (30) and bound $\|\nu_\omega(t)\|^2$ and $\|\nu_u(t)\|^2$ by $\|\nu_\omega(\cdot)\|_\infty^2$ and $\|\nu_u(\cdot)\|_\infty^2$, which yields

$$\begin{aligned}W(t) \leq & e^{-\frac{1}{2}\hat{\alpha} t} W(0) \\ & + \mu_1 \|\nu_\omega(\cdot)\|_\infty^2 + \mu_2 \|\nu_u(\cdot)\|_\infty^2,\end{aligned} \tag{31}$$

after which it follows from a double application of Lemma 1 that

$$\begin{aligned}\|x_\mathbf{G}(t)\|^2 \leq & \frac{\bar{c}}{\underline{c}} e^{-\hat{\alpha} t} \|x_\mathbf{G}(0)\|^2 \\ & + \frac{\mu_1}{\underline{c}} \|\nu_\omega(\cdot)\|_\infty^2 + \frac{\mu_2}{\underline{c}} \|\nu_u(\cdot)\|_\infty^2.\end{aligned} \tag{32}$$

This result leaves the load frequencies unaccounted for. It is possible to take them into account, by recalling that the initial condition $x(0)$ satisfies (8c). We define X such that this condition on $\omega_\mathbf{L}(0)$ is met. Then,

$$\begin{aligned}\|\omega_\mathbf{L}\|^2 &\leq \|D_\mathbf{L}{}^{-1}(\nabla U(\delta) - \nabla U(\bar{\delta}))_\mathbf{L}\|^2 \\ &\leq \lambda_{\max}(D^{-2})\|\nabla U(\delta) - \nabla U(\bar{\delta})\|^2 \\ &\leq \alpha_2 \lambda_{\max}(D^{-2})\|\delta - \bar{\delta}\|^2,\end{aligned} \tag{33}$$

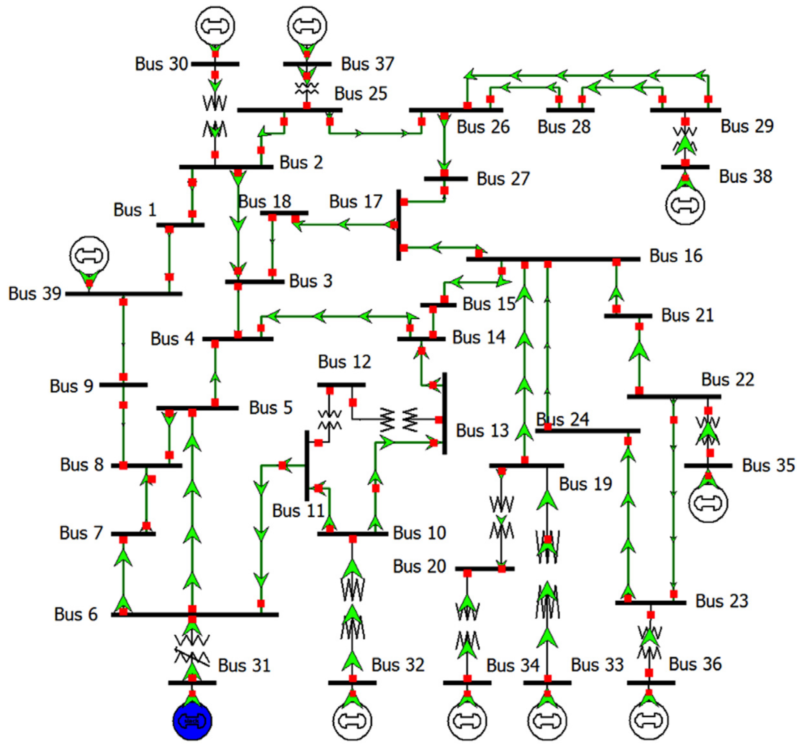

Fig. 1. The structure of the IEEE 39 New England benchmark network.

where the last inequality follows from Statement 1 of Lemma 4 in Weitenberg et al. [12]. As a result,

$$\|x(t)\|^2 \le \frac{\bar{c}}{\underline{c}} e^{-\hat{\alpha}t}(1+\alpha_2\lambda_{\max}(D^{-2}))\|x(0)\|^2 + \gamma_1\|\nu_\omega(\cdot)\|_\infty^2 + \gamma_2\|\nu_u(\cdot)\|_\infty^2. \quad (34)$$

In the above, we have set $\gamma_i := \mu_i(\alpha_2\lambda_{\max}(D^{-2})+1)/\underline{c}$, $i = 1,2$. We therefore conclude that the theorem holds with $\lambda := \frac{\bar{c}}{\underline{c}}(1+\alpha_2\lambda_{\max}(D^{-2}))$. $\square$

Remark 2. It is worthwhile to observe that a slight variation of the previous analysis shows that the uncontrolled Bergen–Hill model is ISS with restrictions with respect to the input disturbance ν_u. To see this, it is enough to neglect the controller dynamics (8d), set $u-\bar{u} = \mathbb{0}$ in (8b) and let $\epsilon_2 = 0$ in the Lyapunov function W. Then, with $x(\delta,\omega) := \mathrm{col}(\delta-\bar{\delta},\omega)$, the analysis above leads to conclude that the solutions satisfy $\|x(\delta(t),\omega(t))\|^2 \le \lambda e^{-\hat{\alpha}t}\|x(\delta(0),\omega(0))\|^2 + \gamma_2\|\nu_u(\cdot)\|_\infty^2$ for all $t \ge 0$, provided that $x(\delta(0),\omega(0)) \in X$, and $\|\nu_u(\cdot)\|_\infty \le N_2$, possibly with different values of the parameters $\lambda, \hat{\alpha}, \gamma_2, N_2$ and a different set X.

4.1. Discussion

For tuning purposes, it is useful to explicitly note the effects of the controller parameters on the convergence and noise rejection. The only parameters are the values Q_i, which are partially fixed by the definition of the cost function $C(u)$ defined in Section 2. However, we note that replacing Q by σQ, with the scaling factor $\sigma \in \mathbb{R}_{>0}$, does not change the equilibrium (7), and therefore leaves the 'true' generation cost unchanged. We investigate the effect of using values $\sigma \neq 1$ on the decay rate $\hat{\alpha}$ and the noise-to-state gains γ_1 and γ_2 appearing in the ISS inequality (29) of Theorem 1.

Exponential decay rate $\hat{\alpha}$. First, consider the parameter $\hat{\alpha} = 2\frac{c'-\mu_0}{\bar{c}}$ in Theorem 1. Assuming that μ_0 is kept constant, and considering that $\bar{c}$ is a non-decreasing function of σ while c' is, for sufficiently small ϵ_2, independent of Q, we conclude that $\hat{\alpha}$ *is a non-increasing function of* σ.

Noise-to-state gains γ_1, γ_2. The parameters γ_1, γ_2 depend on $\underline{c}$, the lower bound parameter given in (11), and on μ_1, μ_2, the Young's inequality parameters defined in (25). Note that $\underline{c}$ is a non-decreasing function of σ.

Using the definition of γ_1 in the proof of Theorem 1, which is $\gamma_1 = \mu_1(\alpha_2\lambda_{\max}(D^{-2})+1)/\underline{c}$, we conclude that it is increasing in the parameter μ_1, which is non-increasing in σ^2. Note that the factor $\alpha_2\lambda_{\max}(D^{-2})+1$ is a constant with respect to σ. As a result, for sufficiently small values of ϵ_2, we conclude that γ_1 *is non-increasing as a function of* σ.

The same holds for $\gamma_2 = \mu_2(\alpha_2\lambda_{\max}(D^{-2})+1)/\underline{c}$; however, since it depends on μ_2 which is independent of σ, the effect of tuning σ on μ_2 is expected to be less pronounced. This is in line with expectations: since actuation noise is added at the controller output, it affects the plant dynamics unfiltered.

Summary. Based on these considerations, we infer that higher values in Q will likely increase robustness to noise by decreasing the noise-to-state gains γ_1, γ_2, whereas they reduce the overall convergence speed $\hat{\alpha}$ of the closed-loop system. However, due to the considerations above, the range of γ_1 and γ_2 as function of σ may be bounded from below. In our simulations, discussed next, this turns out not to be an issue, as using such high values of σ reduce the convergence speed past the point where the control action is useful.

4.2. Case study

As a case study, we use the 39-node IEEE 'New England' benchmark, the network structure of which is depicted in Fig. 1. For this case study, we have equipped all 10 generation units with a DAI controller. The relative values of Q_i have been chosen in such a way

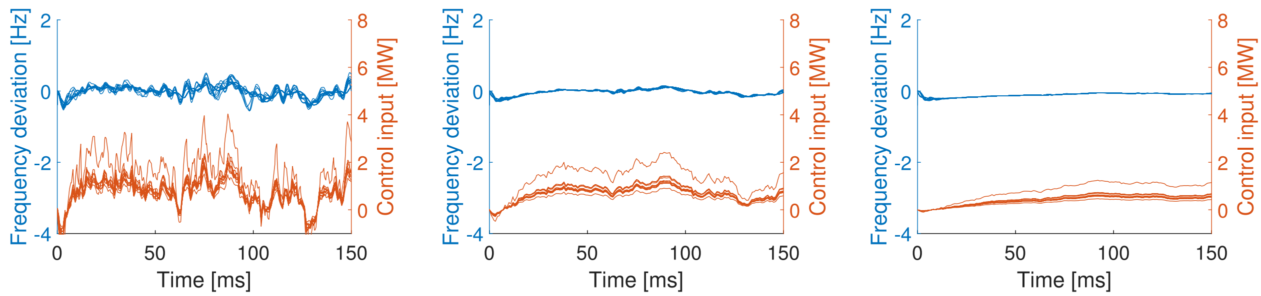

(a) Q decreased by factor 5 (b) Nominal values of Q (c) Q increased by factor 5

Fig. 2. Simulations of the IEEE 39-bus New England system, with a complete communication graph. The system is initialized without demand, and at $t = 0$ the loads are turned on. The same noise is applied each time to the measurements and communication, but the cost function $C(u) = u^\top Qu$ is scaled by an increasing factor. Note how measurement noise is rejected more effectively, but convergence is slower, as values of Q increase.

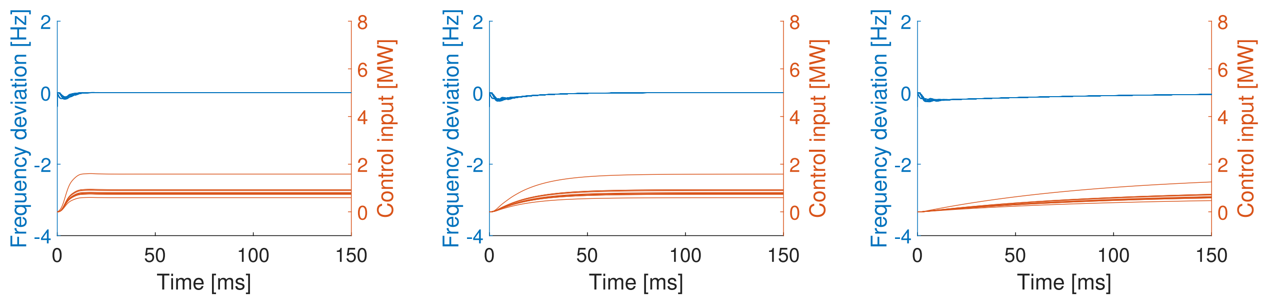

(a) Q decreased by factor 5 (b) Nominal values of Q (c) Q increased by factor 5

Fig. 3. Same simulation as in Fig. 2, but without any noise, for comparison.

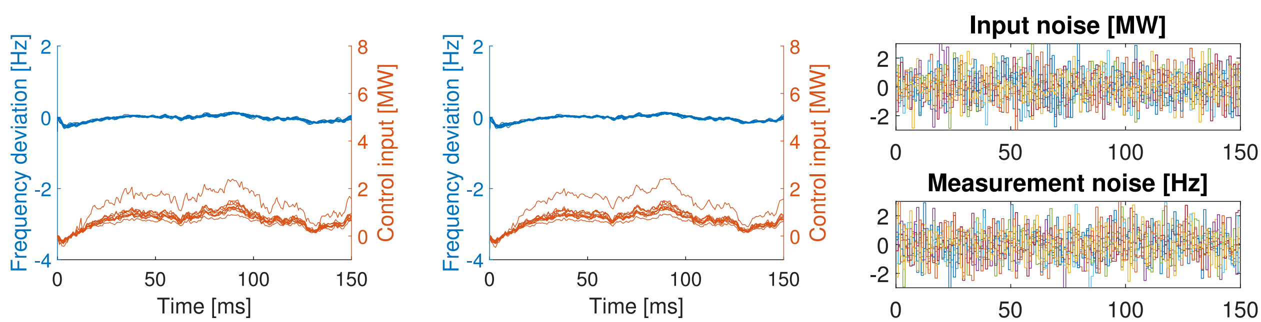

(a) $\mathcal{L}_u$ represents a circle graph (b) $\mathcal{L}_u$ represents a star graph (c) Noise used in the simulations

Fig. 4. Simulations of the IEEE 39-bus New England system, this time with different communication topologies.

as to lead to balanced performance, with the relative weight of the generators decided arbitrarily.

For each simulation, the network was initialized without demand. At time $t = 0$, each node was assigned an arbitrary load, the same for each simulation. The evolution of the closed-loop system was then measured. In the simulations with noise, a randomly distributed piecewise constant noise function was used (again the same for each simulation). Since the actuator usually resides at the plant actuation noise is disregarded except in Fig. 5.

To highlight the role of the network parameters in the ISS gain of the noise, as evidenced by (22), we show the evolution of the system in Fig. 2 (compare Fig. 3) for the nominal value of Q as well as with Q scaled up and down by a factor 5. Note that the effect of Q is clearly visible in the injected power by the nodes. Additionally, these simulations illustrate the presence of a trade-off described earlier between a fast controller performance, for lower values of Q, and more effective rejection of noise, for higher values.

Additionally, we compare the effects of using a circle graph or a line graph as the communication topology (instead of a complete graph) in Fig. 4. Though, as expected from the definition of $\hat{\alpha}$ in Theorem 1, the convergence speed is slower for more sparse graphs, noise rejection is not affected much by the communication topology.

Finally, in Fig. 6 we show the root mean squared error (RMSE) of the frequency deviation at $t = 150$ ms, scaling Q by the scale factor σ. Note that for $\sigma \to 0$ (and therefore $Q_i \to 0$), the robustness of the system to noise vanishes, as predicted. Large values of σ lead to robustness, but the system converges more slowly, as evidenced by the fact that the RMSE at 150 ms rises for larger values.

5. Conclusions

Finally, we summarize our results and observations and discuss the aspects that should be taken into account when tuning a DAI controller.

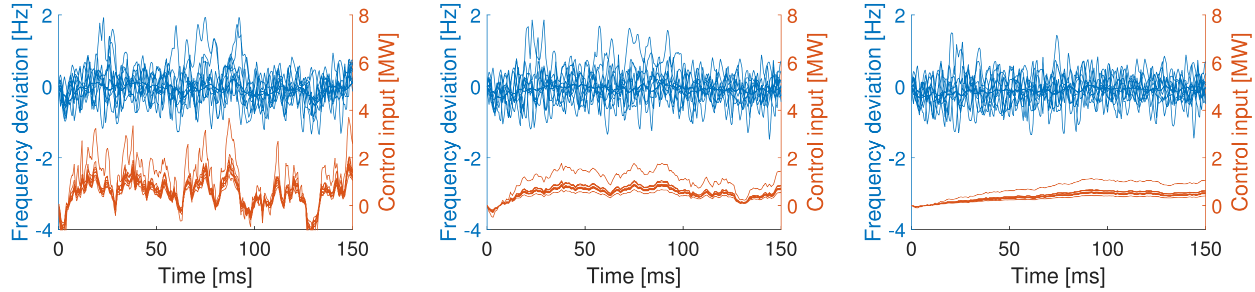

(a) Q decreased by factor 5 (b) Nominal values of Q (c) Q increased by factor 5

Fig. 5. Simulations of the IEEE 39-bus New England system, this time with noise on actuation in addition to measurements and communication. Since actuation noise enters $\dot{\omega}$ at the control input, it is more visible in ω, but its effect is filtered out of u.

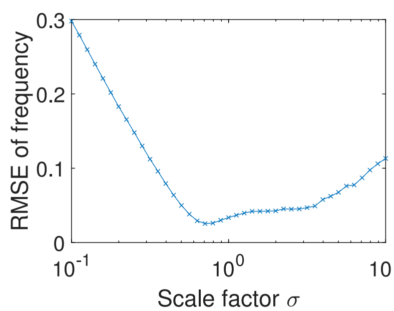

Fig. 6. Same simulation as in Fig. 2, with Q replaced by σQ. The root mean squared error (RMSE) of the frequency is plotted versus σ.

As shown in Theorem 1, the DAI controller is input-to-state stable, with respect to supremum-bounded noise in measurements, communication and actuation. We find therefore that the DAI controller combines the attractive properties of frequency regulation and economic optimality with robustness.

The DAI controller can be tuned via its weight variable Q. The relative magnitude of the elements Q_i are used to achieve optimal dispatch. However, multiplication by a factor does not affect $\bar{u}$ as seen from (7), while the local convergence behavior and robustness to noise is affected.

Naively, the edge cases $Q_i \to 0$ and $Q_i \to \infty$ result in pure integral control and an open loop, respectively. Pure integral control offers perfect frequency regulation, but no optimal dispatch or robustness to noise. Open loop control, having no frequency measurements, does not offer frequency regulation at all.

These edge cases correspond with our findings. Specifically, from Theorem 1, we conclude that low values of Q result in a higher rate of convergence to the synchronous solution, but also a higher noise-to-state gain, i.e. less robustness. Conversely, high values of Q result in a lower rate of convergence, but a lower noise-to-state gain, therefore more robustness to noise.

It is worth noting that the ISS gains γ_1, γ_2, the decay rate $\hat{\alpha}$ and restrictions N_1, N_2 and X are likely to be conservative compared to the behavior of the system. This is due to the fact that we take the minimum decay rate for states in a level set of the Lyapunov function; reducing the permissible state values should improve the tightness of the bounds. This was also discussed in Weitenberg et al. [12].

In conclusion, the DAI controller offers perfect frequency regulation and optimal dispatch when applied to the swing equations, as well as any other network of nonlinear systems as noted in Remark 1. Though its transient performance and ISS-style robustness to noise are at odds with each other, once can reduce the effect of noise on the power injections by tuning Q.

References

[1] T. Stegink, C. De Persis, A. van der Schaft, A unifying energy-based approach to stability of power grids with market dynamics, IEEE Trans. Automat. Control 62 (6) (2017) 2612–2622.
[2] N. Li, L. Chen, C. Zhao, S.H. Low, Connecting automatic generation control and economic dispatch from an optimization view, in: American Control Conference (ACC), 2014, pp. 735–740.
[3] X. Zhang, A. Papachristodoulou, A real-time control framework for smart power networks with star topology, in: American Control Conference (ACC), 2013, pp. 5062–5067.
[4] M. Bürger, C. De Persis, S. Trip, An internal model approach to (optimal) frequency regulation in power grids, in: 21st International Symposium on Mathematical Theory of Networks and Systems, 2014, pp. 577–583.
[5] S. Trip, M. Bürger, C. De Persis, An internal model approach to (optimal) frequency regulation in power grids with time-varying voltages, Automatica 64 (2016) 240–253.
[6] J.W. Simpson-Porco, F. Dörfler, F. Bullo, Synchronization and power sharing for droop-controlled inverters in islanded microgrids, Automatica 49 (9) (2013) 2603–2611.
[7] C. De Persis, N. Monshizadeh, Bregman storage functions for microgrid control, IEEE Trans. Automat. Control (2017).
[8] F. Dörfler, J.W. Simpson-Porco, F. Bullo, Breaking the hierarchy: Distributed control and economic optimality in microgrids, IEEE Trans. Control Netw. Syst. 3 (3) (2016) 241–253.
[9] H. Flamme, E. Tegling, H. Sandberg, Performance limitations of distributed integral control in power networks under noisy measurements, 2017, arXiv:1709.08893.
[10] X. Wu, F. Dörfler, M.R. Jovanović, Topology identification and design of distributed integral action in power networks, in: 2016 American Control Conference, IEEE, 2016.
[11] M. Andreasson, D.V. Dimarogonas, H. Sandberg, K.H. Johansson, Distributed PI-control with applications to power systems frequency control, in: 2014 American Control Conference (ACC) June 4-6, 2014, IEEE, Portland, Oregon, USA, 2014.
[12] E. Weitenberg, C. De Persis, N. Monshizadeh, Quantifying the performance of optimal frequency regulators in the presence of intermittent communication disruptions, IFAC-PapersOnLine 50 (1) (2017) 1686–1691, 20th IFAC World Congress. An unabridged version is available as arXiv:1608.03798 with the title "Exponential convergence under distributed averaging integral frequency control".
[13] E. Weitenberg, Y. Jiang, C. Zhao, E. Mallada, C. De Persis, F. Dörfler, Robust decentralized secondary frequency control in power systems: Merits and trade-offs, under review, 2018, arXiv:1711.07332v1.
[14] A. Bergen, D.J. Hill, A structure preserving model for power system stability analysis, IEEE Trans. Power Appar. Syst. (1) (1981) 25–35.
[15] P. Kundur, N.J. Balu, M.G. Lauby, Power System Stability and Control, Vol. 7, McGraw-hill, New York, 1994.
[16] M. Arcak, Passivity as a design tool for group coordination, IEEE Trans. Automat. Control 52 (8) (2007) 1380–1390.
[17] F. Dörfler, M. Chertkov, F. Bullo, Synchronization in complex oscillator networks and smart grids, Proc. Natl. Acad. Sci. 110 (6) (2013) 2005–2010.
[18] N. Monshizadeh, C. De Persis, Agreeing in networks: unmatched disturbances, algebraic constraints and optimality, Automatica (75) (2017) 63–74.
[19] H. Khalil, in: M.J. Horton (Ed.), Nonlinear Control, Pearson, 2014.